Int J CARS (2017) 12:803–809
DOI 10.1007/s11548-016-1485-1

ORIGINAL ARTICLE

Evaluation of a robotic system for irreversible electroporation (IRE) of malignant liver tumors: initial results

L. P. Beyer[1] · B. Pregler[1] · K. Michalik[1] · C. Niessen[1] · M. Dollinger[1] · M. Müller[2] · H. J. Schlitt[3] · C. Stroszczynski[1] · P. Wiggermann[1]

Received: 16 January 2016 / Accepted: 1 September 2016 / Published online: 21 September 2016

Abstract
Objective Comparison of conventional CT-guided manual irreversible electroporation (IRE) of malignant liver tumors and a robot-assisted approach regarding procedural accuracy, intervention time, dose, complications, and treatment success.
Methods A retrospective single-center analysis of 40 cases of irreversible electroporation of malignant liver tumors in 35 patients (6 females, 29 males, average age 60.3 years). Nineteen of these ablation procedures were performed manually and 21 with robotic assistance. A follow-up (ultrasound, CT, and MRI) was performed after 6 weeks in all patients.
Results The time from the planning CT scan to the start of the ablation as well as the dose-length product were significantly lower under robotic assistance (63.5 vs. 87.4 min, $p < 0.001$; 2132 vs. 4714 mGy cm, $p < 0.001$). The procedural accuracy, measured as the deviation of the IRE probes with respect to a defined reference probe, was significantly higher using robotic guidance (2.2 vs. 3.1 mm, $p < 0.001$). There were no complications. There was one incomplete ablation in the manual group.
Conclusion Robotic assistance for IRE of liver tumors allows for faster procedure times with higher accuracy while reducing radiation dose as compared to the manual placement of IRE probes.

✉ L. P. Beyer
lukas@lukasbeyer.com

[1] Department of Radiology, University Medical Center Regensburg, 93053 Regensburg, Germany

[2] Department of Internal Medicine I, University Medical Center Regensburg, Regensburg, Germany

[3] Department of Surgery, University Medical Center Regensburg, Regensburg, Germany

Keywords Interventional radiology · Robotic assistance · Irreversible electroporation · Liver tumor · CT-guided

Introduction

Approximately 70 % of liver metastases are considered non-resectable at the time of their diagnosis, partly due to their anatomical location and partly due to comorbidities or limited liver function. In the case of unresectability, thermal ablation via radio frequency ablation (RFA) and microwave ablation (MWA) is the treatment of choice [1–3].

The fact that both methods (RFA and MWA) cannot be used or can only be used on a limited basis in the proximity of heat-sensitive structures, such as the stomach and gallbladder, are considered a limitation. In addition, incomplete ablation can occur in the case of thermal ablation in the vicinity of larger vascular structures due to the dissipation of heat caused by blood flow (often referred to as the heat sink effect) [4–6].

Irreversible electroporation (IRE) has become established in recent years as a non-thermal alternative to RFA and MWA [7]. IRE is based on the increase in the permeability of cell membranes with respect to ions, proteins, and DNA [8]. The cell membrane is damaged to such an extent that the cell cannot recover and suffers apoptotic or necrotic cell death only if the electrical field is sufficiently strong [9,10]. IRE protects heat-sensitive structures and also allows the ablation of tumors in the immediate vicinity of large vascular structures [11,12].

In contrast to thermal methods in which only one needle is usually placed in the tumor center, 2–6 needles must be placed exactly in parallel and at precisely defined distances in and around the tumor in the case of IRE. Application of a sufficiently strong electrical field to the entire tumor

requires exact placement of the electrodes [13,14]. Mathematical models have shown that an even distribution of the electromagnetic field highly depends on the parallel placement of IRE electrodes [15] and directly affects therapeutic efficacy of IRE ablations [16]. Needle positioning requires significant experience and can represent a substantial challenge for interventionalists in the case of tumors that are hard to visualize and difficult access paths. Needles can be placed under ultrasound or CT guidance with CT guidance being commonly used as intervention time is significantly shorter and access to the tumor location is often difficult.

In the case of thermal methods, there are already multiple studies showing that modern CT-based navigation systems allow exact planning of the access path and precise placement of the ablation probe [18,19]. To the knowledge of the authors, there are not yet any studies examining the use of such navigation systems in IRE. Therefore, we report our results from a comparison of a novel robotic system to the CT-guided fluoroscopic manual approach for needle positioning in IRE of malignant liver tumors.

Materials and methods

Study design, participant selection, and patient characteristics

The radiological data and intervention protocols of all IRE procedures conducted at our institute between August 2014 and August 2015 were included in a retrospective observational study. The indication for percutaneous tumor ablation was determined in all cases by an interdisciplinary tumor board. IRE was indicated when surgical resection was not possible and RFA or MWA was contraindicated due to the proximity of the tumor to heat-sensitive structures or vessels. Exclusion criteria were resectability of the tumor, a relevant coagulation disorder, general anesthesia contraindications, and a tumor situation that could no longer be locally managed by ablation because of size and/or number of lesions.

In total, data from 40 cases of irreversible electroporation of primary liver tumors or liver metastases in 35 patients (6 females, 29 males, average age 60.3 years, age range 46–78 years) treated by IRE were collected. The project was initially conducted as an evaluation of a commercially available robotic device, Maxio (Perfint Healthcare, Florence, Oregon, USA). The first 19 procedures were performed using CT fluoroscopy; the other 21 procedures using robotic assistance. In all cases, a preinterventional MRI examination using liver-specific contrast agent (Primovist, Bayer Schering Pharma, Berlin) was available as a reference image. Eighteen of the 40 ablated lesions were hepatocellular carcinomas, and the remaining 22 were liver metastases (Table 1).

Table 1 Number of lesions ablated under CT fluoroscopy or robotic guidance

	Manual	Guided
Hepatocellular carcinoma	11	7
Metastasis		
Colorectal cancer	8	10
Breast cancer	0	2
Pancreatic cancer	0	2
All	19	21

IRE procedure

All IRE ablations were performed under general anesthesia by an experienced interventional radiologist using the NanoKnife System (AngioDynamics®, Latham, New York)

For IRE planning, a three-phase CT scan (Somatom Sensation 16, Siemens Healthcare, Forchheim, Germany) of the liver during breath-hold was performed immediately before the intervention. Contrast-enhanced arterial phase images were generated during injection of 120 mL of nonionic contrast material at a flow rate of 4 mL/sec using bolus tracking with a threshold of 100 HU. Portal venous phase images were obtained 50 s after the arterial phase scan.

The number and position of needles needed to ablate the tumor completely and with a safety distance of 1 cm was determined with the NanoKnife system based on the size and shape of the tumor. The electrodes were placed anterior–posterior in all cases.

A non-contrast control scan was performed in all cases after placement of the needles to determine the exact distances between the needles.

Manual approach

CT fluoroscopy (CARE Vision, Somatom Sensation 16, Siemens Healthcare, Forchheim, Germany; CT parameters during fluoroscopy: tube voltage 120 kVp; effective tube current-time product 30 mAs; slice collimation 16 mm × 0.75 mm) is an acquisition mode that allows continuous image update using in-room table control. After the initial 3-phase planning CT scan, 2–6 monopolar 18-gauge ablation electrodes were placed parallel to each other at a defined distance depending on anatomy and tumor size. CT fluoroscopy was used for repeated checking of the needle position until all needles were placed in the required position either around or in the target tumor. Additional spiral CT scans of the liver were performed in all cases during the intervention to check probe position.

Robotic guidance

Before robot-assisted image-guided tumor ablation, all patients were positioned on a vacuum mattress to minimize patient movability between the planning multi-slice CT scan and robot-assisted positioning of the ablation electrodes. After performing a 3-phase CT scan of the liver, the data set was sent to the workstation, Maxio (Perfint Healthcare, Florence, Oregon, USA); Table 2. The included planning software performs bone detection and semi-automatic liver segmentation including liver vessels. Afterward, the tumor was manually marked and segmented by the software.

The entry point of each ablation electrode in the skin and the target points in and around the tumor were determined to plan the access path. During planning, warnings are issued automatically if the needle path intersects critical structures, especially liver vessels and bones. After approval of the plan by the interventionalist, the robotic arm is automatically positioned over the patient (Fig. 1). The stereotactic arm takes about 30 s to move to the final position. In this way, the puncture direction and depth are specified by the robot on the basis of the previously determined plan. The IRE needle is then inserted through the needle applicator at the end of the effector of the robotic arm. This step is repeated for every ablation electrode. Additional spiral CT scans of the liver were performed in all cases during the intervention to check probe position. If the performing physician deemed needle position inadequate, i.e., needle deviation or close proximity to adjacent organs, manual correction was performed.

Radiation exposure dose

The total dose-length product (total DLP), fluoroscopy DLP, verification DLP, and the number of verification scans to check the location of the needle during the intervention were recorded.

Table 2 Technical specification of the robotic system

Physical attributes	
Height/width/depth	1310/775/850 mm
Weight	250 kg
Positioning of the device	Registration on the floor
Mechanical Specification	
X/Y/Z range	600/450/180 mm
A/B range	±95°
Compatible needles	
Thickness	11–22 Gauge
Length	60–250 mm

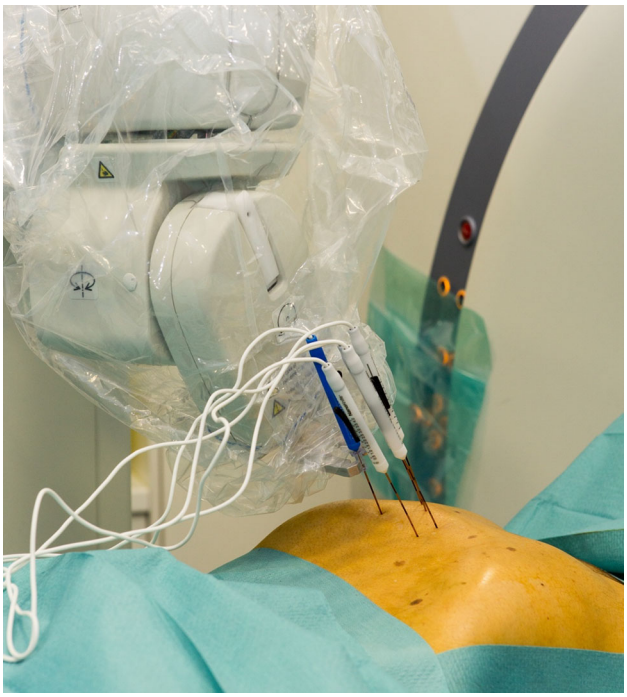

Fig. 1 Positioning of the robotic arm for placement of the IRE electrodes

Procedural accuracy

For objective evaluation of the parallelism of the ablation electrodes, the probe in the most central position in the tumor was defined as the reference electrode. A thin-slice (slice thickness 0.7 mm) reconstruction orthogonal to the reference electrode was then performed for every patient. Based on this reconstruction, the lateral deviation with respect to the reference electrode over the last 3 cm (from the probe tip) was measured for each additional probe (Fig. 2). If manual position correction was necessary, the deviation was measured before the repositioning.

Complications

Complications were documented and classified as minor and major according to the standardized grading system of the Society of Interventional Radiology [20].

Follow-up

All patients underwent a 6-week follow-up including an MRI scan with liver-specific contrast agent as well as a 3-phase computed tomography scan of the liver. The ablation volume measured in the axial plane and the radiographic evaluation/visual assessment of the complete success of the ablation were analyzed by two experienced radiologists. Long-term follow-up was performed only by MRI if short-term follow-up showed complete ablation without complications.

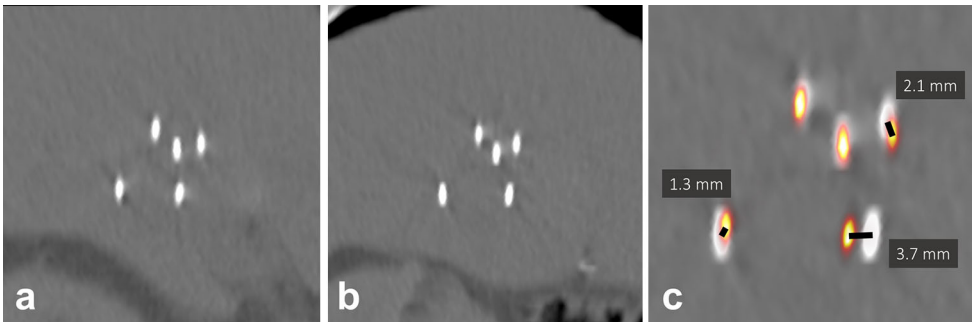

Fig. 2 Reconstruction to determine the lateral deviation of the IRE electrodes. **a** Reconstruction (slice thickness 0.7 mm) orthogonal to and at the tip of the reference electrode. **b** Reconstruction orthogonal to the reference electrode at a distance of 3 cm from the tip of the electrode. **c** MIP (maximum intensity projection) from (**a**) and (**b**) with determination of the lateral probe deviations

Statistical analysis

The JMP statistics software package (SAS Institute, Cary, NC, USA) was used to perform all statistical calculations. A p value of $p \leq 0.05$ was considered the cut-off point of statistical significance. Normality was verified according to statistical parameters (mean, median, skewness, and kurtosis). Paired abnormally distributed data were compared with the Mann–Whitney U test. The Chi-squared test was used to test for independence of categorical variables.

Results

Tumor characteristics

Lesion aspects are summarized in Table 3. There were no clinical or statistical differences between both groups regarding the tumor characteristics.

Procedural accuracy

The average deviation of the IRE electrodes with respect to the reference electrode (Fig. 3) was 3.1 mm (range 0.2–6.2 mm, SD 1.2) for manual placement and 2.2 mm (range 0.0–4.0 mm, SD 1.0) for navigation-assisted placement with the difference being statistically significant ($p < 0.001$).

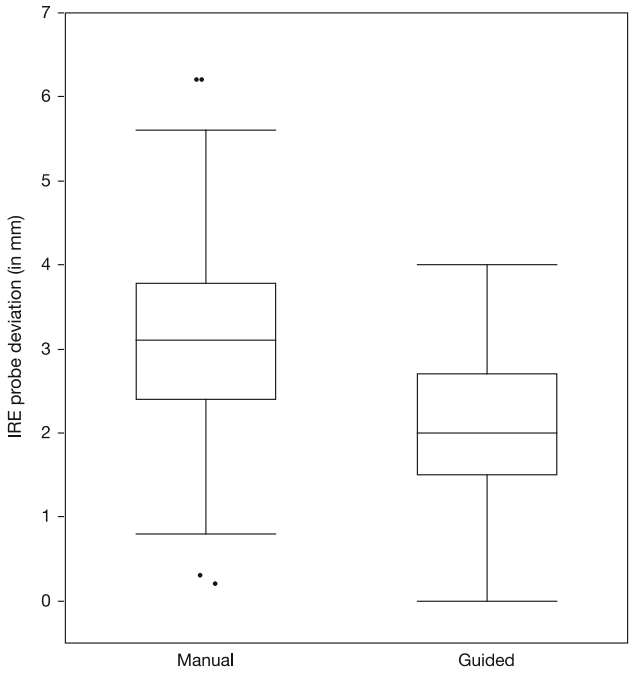

Fig. 3 Average deviation of IRE electrodes with respect to the reference electrode over the last 3 cm from the probe tip

Table 3 Lesion aspects

Manual or guided	Manual ($N = 19$)	Guided ($N = 21$)	p
Skin to tumor depth (mm)	79.1 ± 26.3	74.7 ± 30.4	0.314
Tumor long axis (mm)	25.8 ± 11.4	24.9 ± 8.7	0.399
Tumor conspicuity native (HU)	11.1 ± 7.5	14.3 ± 16.7	0.785
Tumor conspicuity enhanced (HU)	35.7 ± 13.7	41.7 ± 23.1	0.841
Number of vessels within a perimeter of 1.0 cm			
Right PV—no. (%)	6 (28.6 %)	6 (28.6 %)	0.84
Left PV—no. (%)	5 (26.3 %)	5 (23.8 %)	0.86
Hepatic vein—no. (%)	4 (21.1 %)	4 (19.0 %)	0.87
Inferior vena Cava—no. (%)	4 (21.1 %)	3 (14.3 %)	0.57

Lesion conspicuity denotes the difference in attenuation between tumor and liver parenchyma

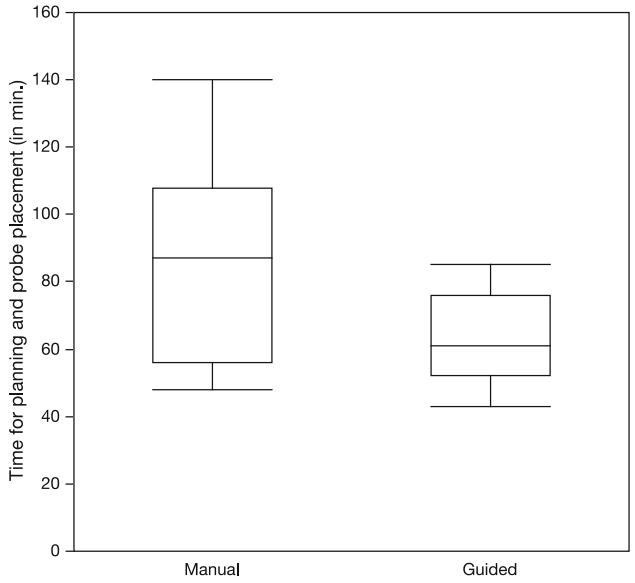

Fig. 4 Average time from planning CT scan to control scan including final electrode position

Procedural duration

During robot-assisted ablation, the average planning time from the planning CT scan to the start of probe positioning was 19.3 min (range 15–26 min, SD 3.2). The average time from the start of placement of the first ablation probe to the final control scan of the final electrode position was 87.4 min (range 48–140 min, SD 27.6) for manual ablation and 44.2 min (range 28–64 min, SD 12.6) for robot-assisted ablation. The total time from the planning scan to the final control scan was significantly shorter in robot-assisted ablation than manual ablation ($p < 0.001$; Fig. 4).

Radiation dose

The total DLP and the fluoroscopy DLP were significantly lower in robot-assisted ablation than manual ablation (Table 4).

Subgroup analysis of robot-assisted ablations

Manual needle repositioning was performed in 7 of 21 cases. The insertion time of the probes, the fluoroscopy DLP, and the number of verification scans were significantly lower when no position correction was necessary (Table 5).

Ablation success

In the follow-up after 6 weeks, complete ablation without residual tumor was seen in 100 % (21 of 21) of robot-assisted ablation cases and in 94.7 % (18 of 19) of manual ablation cases. The difference was not statistically significant ($p = 1$).

Complications

There were no complications in robot-assisted and manual ablation.

Discussion

The goal of the present study was to evaluate robot-assisted percutaneous IRE of malignant liver tumors as a promising alternative to conventional percutaneous IRE under CT fluoroscopy.

Mbalisike et al. [18] were able to show in a prospective study including 70 patients that robot-assisted percutaneous microwave ablation is extremely accurate. Therefore, their measurements yielded only a minimal average deviation of the active center of the microwave probe with respect to the tumor center of 1.9 mm. In a similar study including 64 ablated liver tumors, we found a comparably low deviation of 1.3 mm [19].

The distance of the probes from the tumor center is not a suitable measurement for determining the accuracy of the placement of the IRE probes since the electrodes are placed not only in the center of the tumor but also in the area surrounding the tumor. Therefore, we determined parallelism measured as the deviation of the probes with respect to a reference electrode in the tumor center over the last 3 cm (measured from the tip of the reference electrode) as an alternative measurement. We were able to show that robot-assisted placement with an average deviation of 2.2 mm compared to 3.1 mm in manual placement guarantees a high degree of parallelism.

The possible amount of deviation from exact parallelism and its impact on therapeutic efficacy remain controversial. In a case report by Scheffer et al. [14] demonstrated effective tumor ablation with electrodes placed non-parallel can be achieved. An article by van den Bos et al. [17] addressed the issue of non-parallel electrode placement in silico in a tissue

Table 4 Dose-length product (DLP) of the total intervention, of CT fluoroscopy, and of all verification scans and the number of verification scans

Manual or guided	Manual ($N = 19$)	Guided ($N = 21$)	p
Total DLP (mGy cm)	4714 ± 1704	2132 ± 626	<0.001
Fluoroscopy DLP (mGy cm)	1714 ± 1573	61 ± 85	<0.001
Verification DLP (mGy cm)	1364 ± 457	543 ± 320	<0.001
No. of verification scans	4.1 ± 1.8	1.4 ± 0.6	<0.001

Table 5 Comparison of cases with and without manual position correction

Manual position correction	No ($N = 14$)	Yes ($N = 7$)	p
Insertion time (min)	36.6 ± 6.7	59.4 ± 5.3	<0.001
IRE probe deviation (mm)	2.1 ± 0.9	2.5 ± 1.1	0.972
Fluoroscopy DLP (mGy cm)	33 ± 84	117 ± 58	0.009
Total DLP (mGy cm)	2057 ± 505	2280 ± 846	0.731
No. of verification scans	1.1 ± 0.27	2.0 ± 0.82	0.007

Insertion time, IRE probe deviation, dose-length product (DLP) of CT fluoroscopy and of the total intervention and the number of verification scans

phantom, where it is possible to see, however by heat development, that at least some energy is going from one electrode to another in the entire area of the ablation. Nevertheless for prediction of ablation area, parallelism is preferable.

Systematic errors, i.e., deviation of all probes in the same direction, cannot be reliably ruled out with determination of parallelism. We therefore consider short-term follow-up (after 6 weeks) to be the best measurement of ablation success. While complete ablation was achieved in all 21 cases (100 %) in robot-assisted ablation, residual tumor was seen in 1 of 19 cases (5.3 %) in manual ablation. This can be attributed to the fact that the selected ablation volume was retrospectively determined to be insufficient given the immediate proximity of the tumor to the gallbladder.

We think that a combination of MRI and CT is important for short-term follow-up (after 6 weeks) to determine ablation success and any complications. Due to the often severe comorbidities in oncological patients, MRI scans can often only be used on a limited basis as a result of ascites and/or motion artifacts which complicates the evaluation of any remaining tumor tissue and complications. If short-term follow-up can show complete and complication-free ablation, further follow-up can be limited to MRI in our opinion.

In our study regarding percutaneous microwave ablation of malignant liver tumors, we were able to show that radiation exposure is significantly reduced by robotic assistance [19]. This is even more significant for robot-assisted IRE since not one but multiple probes must be placed. Particularly, significant differences were seen in the case of the DLP resulting from the use of CT fluoroscopy (Table 3). Even though in 7 of 21 cases (33.3 %) the position of the electrodes had to be corrected in the robot-assisted group, the DLP was still significantly lower in comparison with the manual group, where every needle had to be placed under CT fluoroscopy.

In robot-assisted IRE, the time-intensive manual placement of ablation electrodes is no longer necessary. Instead, the robotic arm is automatically positioned over the patient in the defined direction of puncture and at the defined distance so that the ablation electrode can be positioned in one continuous movement. In studies regarding robot-assisted percutaneous microwave ablation in which only one probe needs to be placed according to the method, only minimal advantages were seen in the robot-assisted group regarding the total intervention time. However, in the present study regarding IRE, a significant time savings could be achieved with robotic assistance (63.5 vs. 87.4 min). We attribute this to the fact that the time-intensive planning of probe position with an increasing number of probes is more than compensated by the faster placement. It should be noted that after completion of data acquisition of the current study, a new software version has been released by the manufacturer which allows automated planning of parallel trajectories which might reduce the planning time even further.

This study has some limitations. At the time of study inception, manual approach for percutaneous IRE had been performed for more than 100 times by the participating physicians, while the robotic device was new. A possible learning curve effect for the robotic device might have biased the results toward the manual approach. The single-center setup and the low number of procedures limit generalization of our results. Another limitation is the retrospective nature of the study. However, we think that we were able to demonstrate within the framework of this study the marked reduction of procedure length while maintaining high ablation success.

Conclusion

In summary, our study suggests that percutaneous IRE of malignant liver tumors robotic assistance is a fast, reliable, and effective alternative to manual CT guidance using fluoroscopy. This is in agreement with previous studies. Robotic assistance has the potential to increase precision and reduce radiation dose for the physician and the patient without increasing the risk of complications.

Compliance with ethical standards

Conflict of interest The authors declare that they have no conflict of interest.

Ethical standard All procedures performed in studies involving human participants were in accordance with the ethical standards of the institutional and/or national research committee and with the 1964 Helsinki Declaration and its later amendments or comparable ethical

standards. This study was evaluated retrospectively. For this type of study, formal consent is not required.

References

1. Lubner MG, Brace CL, Hinshaw JL, Lee FT Jr (2010) Microwave tumor ablation: mechanism of action, clinical results, and devices. J Vasc Interv Radiol 21:S192–203. doi:10.1016/j.jvir.2010.04.007
2. Shibata T, Niinobu T, Ogata N, Takami M (2000) Microwave coagulation therapy for multiple hepatic metastases from colorectal carcinoma. Cancer 89:276–284
3. Tanaka K, Shimada H, Nagano Y, Endo I, Sekido H, Togo S (2006) Outcome after hepatic resection versus combined resection and microwave ablation for multiple bilobar colorectal metastases to the liver. Surgery 139:263–273. doi:10.1016/j.surg.2005.07.036
4. Goldberg SN, Hahn PF, Tanabe KK, Mueller PR, Schima W, Athanasoulis CA, Compton CC, Solbiati L, Gazelle GS (1998) Percutaneous radiofrequency tissue ablation: does perfusion-mediated tissue cooling limit coagulation necrosis? J Vasc Interv Radiol 9:101–111
5. Lu DSK, Raman SS, Vodopich DJ, Wang M, Sayre J, Lassman C (2002) Effect of vessel size on creation of hepatic radiofrequency lesions in pigs: assessment of the "heat sink" effect. AJR Am J Roentgenol 178:47–51. doi:10.2214/ajr.178.1.1780047
6. Lu DSK, Yu NC, Raman SS, Limanond P, Lassman C, Murray K, Tong MJ, Amado RG, Busuttil RW (2005) Radiofrequency ablation of hepatocellular carcinoma: treatment success as defined by histologic examination of the explanted liver. Radiology 234:954–60. doi:10.1148/radiol.2343040153
7. Kingham TP, Karkar AM, D'Angelica MI, Allen PJ, DeMatteo RP, Getrajdman GI, Sofocleous CT, Solomon SB, Jarnagin WR, Fong Y (2012) Ablation of perivascular hepatic malignant tumors with irreversible electroporation. J Am Coll Surg 215:379–387. doi:10.1016/j.jamcollsurg.2012.04.029
8. Davalos RV, Mir ILM, Rubinsky B (2005) Tissue ablation with irreversible electroporation. Ann Biomed Eng 33:223–31
9. Yarmush ML, Golberg A, Serša G, Kotnik T, Miklavčič D (2014) Electroporation-based technologies for medicine: principles, applications, and challenges. Annu Rev Biomed Eng 16:295–320. doi:10.1146/annurev-bioeng-071813-104622
10. Jiang C, Davalos RV, Bischof JC (2015) A review of basic to clinical studies of irreversible electroporation therapy. IEEE Trans Biomed Eng 62:4–20. doi:10.1109/TBME.2014.2367543
11. Lee EW, Chen C, Prieto VE, Dry SM, Loh CT, Kee ST (2010) Advanced hepatic ablation technique for creating complete cell death: irreversible electroporation. Radiology 255:426–33. doi:10.1148/radiol.10090337
12. Rubinsky B, Onik G, Mikus P (2007) Irreversible electroporation: a new ablation modality-clinical implications. Technol Cancer Res Treat 6:37–48
13. Martin RCG (2013) Irreversible electroporation of locally advanced pancreatic head adenocarcinoma. J Gastrointest Surg 17:1850–1856. doi:10.1007/s11605-013-2309-z
14. Scheffer HJ, Melenhorst MCAM, Vogel JA, van Tilborg AAJM, Nielsen K, Kazemier G, Meijerink MR (2015) Percutaneous irreversible electroporation of locally advanced pancreatic carcinoma using the dorsal approach: a case report. Cardiovasc Intervent Radiol 38:760–5. doi:10.1007/s00270-014-0950-x
15. Edd JF, Davalos RV (2007) Mathematical modeling of irreversible electroporation for treatment planning. Technol Cancer Res Treat 6:275–86. doi:10.1177/153303460700600403
16. Ben-David E, Ahmed M, Faroja M, Moussa M, Wandel A, Sosna J, Appelbaum L, Nissenbaum I, Goldberg SN (2013) Irreversible electroporation: treatment effect is susceptible to local environment and tissue properties. Radiology 269:738–47. doi:10.1148/radiol.13122590
17. van den Bos W, Scheffer HJ, Vogel JA, Wagstaff PGK, de Bruin DM, de Jong MC, van Gemert MJC, de la Rosette JJMCH, Meijerink MR, Klaessens JH, Verdaasdonk RM (2016) Thermal energy during irreversible electroporation and the influence of different ablation parameters. J Vasc Interv Radiol 27:433–443. doi:10.1016/j.jvir.2015.10.020
18. Mbalisike EC, Vogl TJ, Zangos S, Eichler K, Balakrishnan P, Paul J (2014) Image-guided microwave thermoablation of hepatic tumours using novel robotic guidance: an early experience. Eur Radiol. doi:10.1007/s00330-014-3398-0
19. Beyer LP, Pregler B, Niessen C, Dollinger M, Graf BM, Müller M, Schlitt HJ, Stroszczynski C, Wiggermann P (2015) Robot-assisted microwave thermoablation of liver tumors: a single-center experience. Int J Comput Assist Radiol Surg 11:253–259. doi:10.1007/s11548-015-1286-y
20. Omary RA, Bettmann MA, Cardella JF, Bakal CW, Schwartzberg MS, Sacks D, Rholl KS, Meranze SG, Lewis CA (2003) Quality improvement guidelines for the reporting and archiving of interventional radiology procedures. J Vasc Interv Radiol 14:S293–S295